Data Based Modeling of Solid Oxide Fuel Cells

Srikanth Kutla

A Thesis Submitted to

Indian Institute of Technology Hyderabad

In Partial Fulfillment of the Requirements for

The Degree of Master of Technology

भारतीय प्रौद्योगिकी संस्थान हैदराबाद

Indian Institute of Technology Hyderabad

Department of Chemical Engineering

July 2015

Declaration

I declare that this written submission represents my ideas in my own words, and where others' ideas or words have been included, I have adequately cited and referenced the original sources. I also declare that I have adhered to all principles of academic honesty and integrity and have not misrepresented or fabricated or falsified any idea/data/fact/source in my submission. I understand that any violation of the above will be a cause for disciplinary action by the Institute and can also evoke penal action from the sources that have thus not been properly cited, or from whom proper permission has not been taken when needed.

(Signature)

Kutla Srikanth

(Kutla Srikanth)

CH13M1006

(Roll No)

Approval Sheet

This thesis entitled **Data Based Modeling of Solid Oxide Fuel Cells** by **Kutla Srikanth** is approved for the degree of Master of Technology from IIT Hyderabad.

Dr. C.S. Sastry (Dept. of Mathematics)
(Chairman)

Dr. Parag D. Pawar (Dept. of Chemical Engg.)
Internal Examiner

Dr. Ketan P. Detroja (Dept. of Electrical Engg.)
External Examiner

Dr. Phanindra Jampana (Dept. of Chemical Engg.)
Adviser

Acknowledgements

First, I would like to express my sincere gratitude to my superviser Dr. Phanindra Jampana who has supported me throughout the project, and helped me in learning the concepts as well as coding. I am also thankful to the Department of Chemical Engineering, IIT Hyderabad and the supervisory committee members, Dr. C.S. Sastry, Dr. Parag D. Pawar and Dr. Ketan P. Detroja for giving me valuable suggestions. I would like thank my research group members Mr. Goutham, Mr. Santhosh and all other people who helped and supported me during the M.Tech course.

Thankyou All

Dedication

To my family

Abstract

Solid oxide fuel cells(SOFC) are energy conversion devices capable of producing clean energy with higher efficiencies. Here we are interested in mathematical modeling of fuel cells which is an essential tool in designing control systems. For this we took the input output data from a model which includes all important physical and chemical processes in a fuel cell. A sinusoidal change in inlet velocity of the fuel is considered as the input and the dynamic response of the system with this particular input is considered as output(current density). Because of the complexities involved in the chemical and electrochemical processes, SOFC is a nonlinear system. To identify this system, we have chosen a wavelet based Non-linear Autoregressive Moving Average Model with exogeneous input(NARX). The functional components of the NARX model expanded in wavelet multiresolution expansion. With this, we obtain a linear-in parameters which can be solved by least squares.

Contents

Chapter 1

Introduction

1.1 Introduction

The world's consumption of energy is increasing tremendously day to day. Inorder to meet the raising demand, alternatives sources are being explored. Such a source gaining prime importance is fuel cell owing to it is environmental friendliness. Fuel cell is a electrochemical device which converts chemical energy into electrical energy. Principle of fuel cells is same as batteries but here the difference is fuel is supplied continuosly.

Fuel cells are of different types [1] namely

- Direct methanol fuel cells(DMFC): It operates at 50-120 C using unreformed liquid methanol as a fuel. Suitable at power ranges between 1-50W.
- Phosphoric acid feul cells(PAFC): It operates at 150-200 C using phosphoric acid as an electrolyte with platinum catalyst. Suitable at power ranges between 25-250kW
- Alkaline fuel cells(AFC): It operates at 23-250 C using potassium hydroxide as an electrolyte. Suitable at power ranges between 12kW.
- Solid oxide fuel cells(SOFC): It operates at high temperature of 1000 C with solid oxide as electrolyte. Suitable at power ranges between 2-100kW.
- Molten carbonate fuel cells(MCFC): It operates at a temperature of 600-750

C with molten alkali carbonate mixture as an electrolyte. Suitable at power ranges between 75-250 kW.

1.2 SOFC Theory

SOFC is an environmental friendly device to generate electricity with high efficiencies. It has advantages like fuel flexibility, reliability, very low levels of green house gas emmisons. An SOFC generally consists of two porous electrodes [2], anode composed of Ni-YSZ cermet and cathode composed of lanthanum strontium manganite. These two electrodes are seperated by a dense electrolyte made up of Yttria stabilized zirconia. The operating principle of SOFC is as follows. At the cathode (air electrode), air is supplied where as at anode (fuel electrode) hydrogen or pre reformed hydrocarbons are supplied. Oxygen in the air combines with the electrons coming from the external circuit resulting the formation of oxide ions. The formed oxide ions migrates through the electrolyte to anode and combines with hydrogen to form water and liberation of electrons. The flow of electrons through anode, current collectors and the external circuit constitutes the electricity.

Oxidation of fuel at anode: $H_2 + O^{2-} \longrightarrow H_2O + 2e^-$

Reduction of oxidant at cathode: $\frac{1}{2}O_2 + 2e^- \longrightarrow O^{2-}$

A basic solid oxide fuel cell is as shown in the figure

1.3 Dynamic Modeling

It is essential to understand the dynamic characteristics of the fuel cell for control and development. Dynamic Modeling describes the dynamic response of fuel cell as a function of time. Here, our main focus is on mathemtical modeling because experimentation with the real systems is difficult and dangerous.

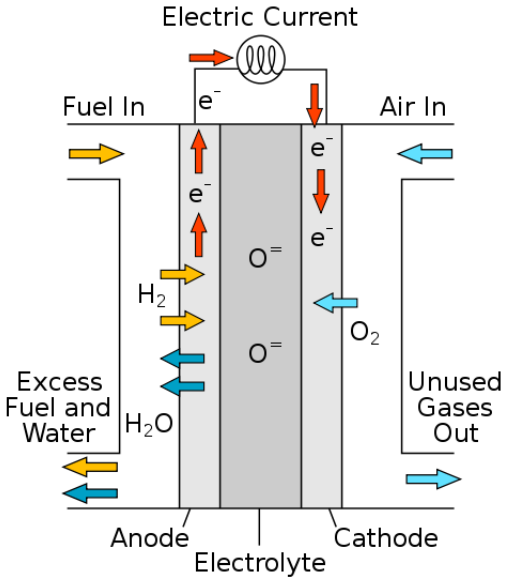

Figure 1.1: Basic Solid Oxide Fuel Cell

Chapter 2

Literature review

Mathematical modeling is an essential tool in developing fuel cells, because of the difficulties involved in experimentation due to its high operating temperature. Due to the complexity involved in the chemical and electrochemical processes, SOFC is considered as nonlinear system, however it is difficult to model this type of systems. Several authors have described a stack model in the past. Few of them including Achenbach [3] presented a computational model on planar SOFC where the temperature and current density distributions were discussed. Zhu [4] developed a physically based modeling framework for SOFC system by considering elementary heterogeneous chemistry, which is much needed for SOFC design.

Later on Colclasure [5] developed a transient model for an anode supported SOFC, where he considered the coupled interactions of fuel flow, electrochemistry, porous media, hear transfer. In this paper, he used system identification techniques to develop the reduced order models. So that these models can be easily included in the process control requirements such as Model predictive control (MPC). In the second part of the colclasure [6] paper continues to use the physically based model, but to extend the reduced models over a large number of operating conditions, a new method Linear Parameter Varying (LPV) is developed. Many of these models are besed on electrochemical kinetics, internal processes such as mass and energy balances. These

models are essentially used for cell design, however it is difficult to use for the control design.

To meet the control strategy requirement, black box modeling is one of the attractive alternatives. This modeling method is based on the input output data without knowledge of the internal structure. Artificial neural networks model is explained in Arriagada [7] using experimental data. Jurado [8] presented a method for the identification of SOFC using a Hammerstein model, comprised of both linear and nonlinear subsystems, used to study the dynamic response. Later, Wavelet analysis, a novel approach in black box modeling has been gained attention. Wavelet analysis can be used in signal processing and system identification and is explained in Mallat [9].

Chapter 3

Deterministic Identification

In deterministic identification algorithm we describe a linear, time invariant, discrete time system in the form of state space models. Where a physical system is represented as a mathematical model in the form of input, output and state variables related by first order differential equations.

3.1 Problem Description

Consider a deterministic system [10] which is having input $u_k \in R^m$ and output $y_k \in R^l$ of order n,

$$x_{k+1}^d = Ax_k^d + Bu_k \tag{3.1}$$

$$y_k = Cx_k^d + Du_k. \tag{3.2}$$

Here the vectors $u_k \in R^m$ and $y_k \in R^l$ are the measurements of the m inputs and l outputs of the process at time instant k . The vector $x_k \in R^n$ is the state vector at discrete time instant k of the process, consists the values of n states.

The matrix $A \in R^{n\times n}$ is the system matrix , $B \in R^{n\times m}$ is the input matrix which influences the next state, $C \in R^{l\times n}$ is the output matrix which describes how

the states are transformed to output measurements y_k and $D \in R^{l \times m}$ is the direct feed through term. Here, our aim is to find out the order n of the system and the system matrices A,B,C,D. Here we use some tools like orthogonal projections.

3.2 Orthogonal Projections

Orthogonal projections are extensively used in our deterministic algorithm.
Projection of row space of a matrix onto the row space of another matrix $B \in R^{q \times j}$ is denoted by an operator π_B .

$$\pi_B = B^T.(BB^T)^\dagger.B \tag{3.3}$$

Here " † " denotes the Moore-Penrose pseudo-inverse of the matrix. If we want to project the row space of a matrix $A \in R^{p \times j}$ onto the row space of matrix B, the expression is as follows.

$$A/B = A.\pi_B \tag{3.4}$$

$$= AB^T.(BB^T)^\dagger.B \tag{3.5}$$

3.2.1 Block hankel matrix

Block hankel matrix plays a vital role in subspace identification. This matrix is constucted from input output data. It is defined as follows,

$$U_{0|2i-1} = \begin{pmatrix} u_0 & u_1 & \cdots & u_{j-1} \\ u_1 & u_2 & \cdots & u_j \\ \cdots & \cdots & \cdots & \cdots \\ u_{i-1} & u_i & \cdots & u_{i+j-2} \\ u_i & u_{i+1} & \cdots & u_{i+j-1} \\ u_i+ & u_{i+2} & \cdots & u_{i+j} \\ \cdots & \cdots & \cdots & \cdots \\ u_{2i-1} & u_{2i} & \cdots & u_{2i+j-2} \end{pmatrix}$$

$$= \frac{U_{0|i-1}}{U_{i|2i-1}} = \frac{U_p}{U_f}$$

Here the number of rows (i) of this matrix is user defined. And it should be greater than the maximum order of the system. Hence this matrix contains a total of 2mi rows. Because each row contains m (number of inputs) rows. The number of columns j equals to s-2i+1, which is the number of data samples used. The subscripts $U_{0|2i-1}$,$U_{0|i-1}$,$U_{0|i}$ denotes the first and last elements of the first column of block hankel matrix. The subscripts p, f stands for past and future. The matrices U_p past inputs and U_f are defined by dividing $U_{0|2i-1}$ into two equal parts which consists of i block rows each. If we shift the border between past and future by one block row down, we get the matrices U_p^+,U_f^- .

3.3 Main Theorem

In this theorem, we discuss how to extract the observability matrix and state sequence from the input output data. The deterministic identification theorem [10] will have two conclusions, they are

• State sequence X_i^d can be computed from input output data without knowing the system matrices.

• The extended observability matrix can be calculated from input-output data.

We will then conclude how to extract these system matrices A,B,C,D from the intermediate results X_i^d and (Γ_i)

3.3.1 Deterministic algorithm

• Oblique projections can be computed using the formulae

$$O_i = Y_f/_{Uf}W_p,$$
$$O_{i-1} = Y_f^-/_{Uf}W_p^+,$$

• Order of the system is determined by the Singular Value Decomposition (SVD) of the weighted oblique projection.

$$W_1 O_i W_2 = USV^T$$

• Here S is the diagonal matrix, by observing singular values in this matrix we can get the order of the system. And dividing the singular value decomposition, we obtain U_1 and S_1.

• Determine the Observability matrix (Γ_i) and (Γ_{i-1}) as

$$\Gamma_i = W_1^{-1}U_1 S_1^{1/2}, \Gamma_{i-1} = \Gamma_i$$

• We can compute the state sequence $X_i^d and X_{i+1}^d$ from

$$X_i^d = \Gamma_i^\dagger O_i$$
$$X_{i+1}^d = \Gamma_{i-1}^\dagger O_{i-1}$$

• By solving a set of equations to get A, B, C, D.

With this deterministic algorithm, we started with a random A,B,C,D matrices as in-

put, output, states. And we identified the system matrices we got from the algorithm are exactly the same matrices which we have chosen randomly.

If we have certain input output data of a particular deterministic system. Assuming random system matrices A,B,C,D By applying deterministic algorithm, finally we are able to get back the system matrices. Now we can compare the assumed system matrices to the matrices which we got through the algorithm. And through the SVD we can get the order of the system. We have done the simulation part in matlab. Following 4 tabular columns represent the assumed values of the system matrices A,B,C,D respectively.

Matrix A:

$$\begin{pmatrix} -1.2660 & 1.58 & -1.9441 & 2.4839 & -0.1987 \\ -0.3102 & 0.1911 & -0.7095 & 0.9252 & -0.1635 \\ -0.3871 & 0.7741 & -1.3036 & 1.153 & -0.3298 \\ -0.6346 & 1.1786 & -1.4315 & 1.3860 & -0.192 \\ -0.4772 & 0.8550 & -1.0574 & 1.2710 & -0.4075 \end{pmatrix}$$

Matrix B:

$$\begin{pmatrix} 0.3683 & 0.2052 & 0.2036 & 0.5480 & 0.4564 & 0.7424 & 0.7590 & 0.5970 & 0.4510 & 0.8270 \\ 0.6556 & 0.4391 & 0.5199 & 0.5669 & 0.0478 & 0.9374 & 0.9933 & 0.4306 & 0.6401 & 0.3081 \\ 0.9382 & 0.0273 & 0.0538 & 0.6804 & 0.7383 & 0.5134 & 0.3567 & 0.7307 & 0.1320 & 0.4024 \\ 0.6204 & 0.8762 & 0.8622 & 0.3714 & 0.0380 & 0.2409 & 0.7529 & 0.2612 & 0.4528 & 0.8842 \\ 0.2828 & 0.6101 & 0.4429 & 0.0782 & 0.9542 & 0.2600 & 0.1100 & 0.0948 & 0.6522 & 0.7006 \end{pmatrix}$$

Matrix C:

$$\begin{pmatrix} 0.2419 & 0.4369 & 0.3972 & 0.1837 & 0.1692 \\ 0.7598 & 0.3043 & 0.4794 & 0.8617 & 0.9522 \\ 0.2909 & 0.2909 & 0.5650 & 0.0326 & 0.5433 \\ 0.2774 & 0.2425 & 0.4896 & 0.3320 & 0.2514 \\ 0.0061 & 0.9367 & 0.2698 & 0.7487 & 0.5786 \\ 0.3747 & 0.8602 & 0.9887 & 0.6444 & 0.9155 \end{pmatrix}$$

Matrix D:

$$\begin{pmatrix} 0.8956 & 0.1319 & 0.2881 & 0.9763 & 0.0018 & 0.6043 & 0.1133 & 0.7981 & 0.9929 & 0.8099 \\ 0.4825 & 0.3559 & 0.2503 & 0.5932 & 0.7118 & 0.5164 & 0.3546 & 0.7956 & 0.1625 & 0.1868 \\ 0.4427 & 0.3959 & 0.4884 & 0.3044 & 0.8677 & 0.0075 & 0.2419 & 0.7811 & 0.1136 & 0.2472 \\ 0.3118 & 0.8855 & 0.7290 & 0.9677 & 0.1183 & 0.6889 & 0.5603 & 0.3511 & 0.9129 & 0.0542 \\ 0.0533 & 0.0212 & 0.2026 & 0.8960 & 0.0390 & 0.9460 & 0.6127 & 0.0543 & 0.4817 & 0.6090 \\ 0.7538 & 0.8441 & 0.2163 & 0.1900 & 0.5982 & 0.8735 & 0.3008 & 0.7087 & 0.8518 & 0.7772 \end{pmatrix}$$

The following 4 matrices represents the result after implementing the deterministic algorithm,

Matrix A new :

$$\begin{pmatrix} 0.1871 & 0.7728 & 0.0581 & -0.0839 & -0.0039 \\ -0.0080 & -0.5472 & -0.0836 & -0.1458 & -0.0063 \\ 0.1215 & 0.04722 & -0.3150 & -0.1591 & -0.0234 \\ 0.0355 & 0.0655 & -0.0199 & -0.3141 & 0.0605 \\ -0.0452 & -0.0040 & -0.0358 & 0.0497 & -0.4108 \end{pmatrix}$$

Matrix B new:

$$\begin{pmatrix} -0.4666 & -0.5565 & -0.5473 & -0.3232 & -0.1890 & -0.4207 & -0.6032 & -0.2463 & -0.4721 & -0.45 \\ 0.1107 & -1.0995 & -1737 & 0.2163 & 1.3740 & 0.0546 & -0.8647 & 0.5569 & -0.4526 & -0.18 \\ 0.2942 & -0.1287 & -0.0708 & 0.2438 & 0.0529 & 0.2657 & 0.1687 & 0.2341 & -0.0019 & -0.11 \\ -0.0081 & 0.2262 & 0.1495 & -0.1243 & 0.3069 & -0.0298 & -0.1267 & -0.1356 & 0.2248 & 0.079 \\ -0.0840 & -0.0288 & -0.0378 & -0.0199 & 0.0576 & 0.1084 & 0.0239 & -0.0149 & 0.0915 & -0.01 \end{pmatrix}$$

Matrix C new:

$$\begin{pmatrix} -1.6504 & 0.2387 & 0.4778 & -0.3006 & 0.3507 \\ -4.3212 & 0.7519 & -1.2375 & -0.4288 & 0.0696 \\ -1.9551 & 0.4726 & 0.2055 & 0.1258 & 0.2638 \\ -1.9369 & 0.3554 & 0.0845 & -0.2861 & -0.3256 \\ -2.8037 & 0.1133 & 0.6325 & 0.333 & 0.0758 \\ -4.3115 & 0.6931 & 0.6206 & 0.1782 & 0.2349 \end{pmatrix}$$

From the matrices D and D new, we can observe that both are similar. The matrices A, B, C which we have chosen initially and the estimated A, B, C are nit same. We need a transformation for this matrices to get the same result.

Matrix D new:

$$\begin{pmatrix} 0.8956 & 0.1319 & 0.2881 & 0.9763 & 0.0018 & 0.6043 & 0.1133 & 0.7981 & 0.9929 & 0.8099 \\ 0.4825 & 0.3559 & 0.2503 & 0.5932 & 0.7118 & 0.5164 & 0.3546 & 0.7956 & 0.1625 & 0.1868 \\ 0.4427 & 0.3959 & 0.4884 & 0.3044 & 0.8677 & 0.0075 & 0.2419 & 0.7811 & 0.1136 & 0.2472 \\ 0.3118 & 0.8855 & 0.7290 & 0.9677 & 0.1183 & 0.6889 & 0.5603 & 0.3511 & 0.9129 & 0.0542 \\ 0.0533 & 0.0212 & 0.2026 & 0.8960 & 0.0390 & 0.9460 & 0.6127 & 0.0543 & 0.4817 & 0.6090 \\ 0.7538 & 0.8441 & 0.2163 & 0.1900 & 0.5982 & 0.8735 & 0.3008 & 0.7087 & 0.8518 & 0.7772 \end{pmatrix}$$

Matrix D:

$$\begin{pmatrix}
0.8956 & 0.1319 & 0.2881 & 0.9763 & 0.0018 & 0.6043 & 0.1133 & 0.7981 & 0.9929 & 0.8099 \\
0.4825 & 0.3559 & 0.2503 & 0.5932 & 0.7118 & 0.5164 & 0.3546 & 0.7956 & 0.1625 & 0.1868 \\
0.4427 & 0.3959 & 0.4884 & 0.3044 & 0.8677 & 0.0075 & 0.2419 & 0.7811 & 0.1136 & 0.2472 \\
0.3118 & 0.8855 & 0.7290 & 0.9677 & 0.1183 & 0.6889 & 0.5603 & 0.3511 & 0.9129 & 0.0542 \\
0.0533 & 0.0212 & 0.2026 & 0.8960 & 0.0390 & 0.9460 & 0.6127 & 0.0543 & 0.4817 & 0.6090 \\
0.7538 & 0.8441 & 0.2163 & 0.1900 & 0.5982 & 0.8735 & 0.3008 & 0.7087 & 0.8518 & 0.7772
\end{pmatrix}$$

Chapter 4

Dynamic model for SOFC

Modelling of Solid oxide fuel cells is important in steady state cell operation in most of the cases. It is also essential to understand the dynamic behaviour to predict the performance of the system. Padulles [11] developed a dynamic model of SOFC which can maitain output voltage. The dynamic model is subjected to varying load current to get steady state output voltage.

4.1 Fuel cell stack model

The following model assumptions are taken from padulles [11] .

4.1.1 model assumptions

- The gases which we will use in this model are considered to be ideal.

- Hydrogen and air are fed to the fuel cell stack. The fuel that we use here is hydrogen.

- Instead of hydrogen if we use natural gas as fuel, the dynamics of the fuel processor should be included.

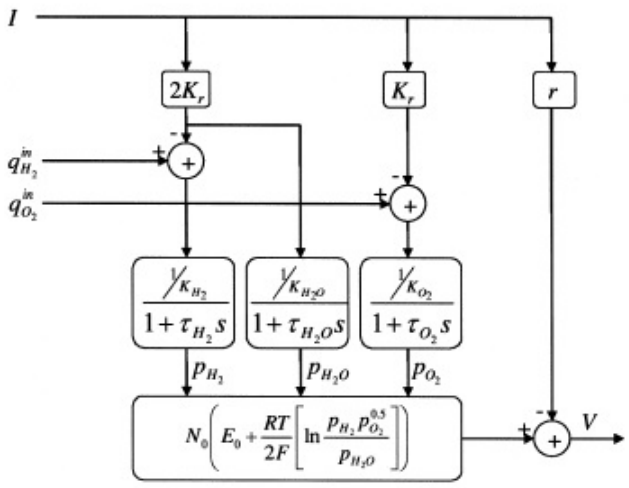

Fig. 2. SOFC stack dynamic model.

Figure 4.1: Fuel Cell stack

- The gases are transported throgh the channels along the electrodes. The volume of the gas channels are fixed however they are small in length.

- In each channel the exhaust gases are sent through a single orifice. The ratio of the interior and exterior presuure of the channel is large. Hence we assume it as choked orifice.

- The temperature is stable at all the times.

- Only ohmic losses are considered.

- Nernst equation can be applied.

4.2 Exhaust gas Characterisation

A gaseous mixture of average molar mass M (kg/kmol) and similar specific heat ratios are fed to a choked orifice. At constant temperature the following characteristics are observed.

$$\frac{W}{P_u} = K\sqrt{M} \tag{4.1}$$

Here W refers to mass flow rate [kg/s], K is the valve constant which depends on the area of the orifice $[\sqrt{k}mol\ kg/(atm\ s)]$, P_u is the pressure upstream inside the channel (atm).

Consider particular case for the anode, here we introduce fuel utilisation U_f concept. It states that the ratio of the fuel that is reacted to the fuel flow injected to the stack. We can also express U_f as the water molar fraction at the exhaust. According to the definition,

$$\frac{W_{an}}{P_{an}} = K_{an}\sqrt{(1-U_f)\ M_{H2}\ + U_f\ M_{H2}o} \tag{4.2}$$

where W_{an} is the mass flow through the anode valve (kg/s); $M_{H2}, M_{H2}o$ are the molecular masses of hydrrogen and water respectively (kg/ kmol).

Here the molar flow of any gas through the valve is proportional to its partial pressure inside the channel,

$$\frac{q_{H2}}{p_{H2}} = \frac{K_{an}}{M_{H2}} = K_{H2} \tag{4.3}$$

and

$$\frac{q_{H2}o}{p_{H2}o} = \frac{K_{an}}{M_{H2}o} = K_{H2}o \tag{4.4}$$

where $q_{H2}, q_{H2}o$ are the molar flows of the hydrogen and water respectively. $p_{H2}, p_{H2}o$ are the partial pressures of hydrogen and water respectively.

The following expression is deduced,

$$\frac{W}{P_u} = K_{an}\,[(1-U_f)\,\sqrt{M_{H_2}}\, + U_f\sqrt{M_{H_2}o}] \tag{4.5}$$

4.3 Calculation of Partial Pressure

The gases we are using are assumed to be ideal. We can apply ideal gas equation, for the case of hydrogen

$$p_{H_2}\,V_{an} = n_{H_2}\,RT \tag{4.6}$$

Here V_{an} is the volume of the anode, n_{H2} is the number of moles of the hydrogen in the anode channel, R is the universal gas constant $[atm/kmol\ T]$, T is the absolute temperature [K]. From the above equation if we write the expression for partial pressure and its derivative is as follows.

$$\frac{d}{dt}\,p_{H_2} = \frac{RT}{V_{an}}\,q_{H_2} \tag{4.7}$$

here q_{H2} is the time derivative of n_{H2} , and represents the hydrogen molar flow rate. Here the hydrogen molar flow constitutes the input flow, output flow and reaction.

$$\frac{d}{dt}\,p_{H_2} = \frac{RT}{V_{an}}\,(q_{H_2}^{in} - q_{H_2}^{o}ut - q_{H_2}^{r}) \tag{4.8}$$

According to the basic electrochemical relationships, the molar flow of hydrogen that reacts can be calculated as :

$$q_{H_2}^{r} = \frac{N_0\,I}{2\,F} = 2\,K_r\,I, \tag{4.9}$$

where N_0 is the number of cells associated in fuel cell stack in series. F is the faraday's constant (C/ kmol),I is the stack current, K_r is a constanat defined for modelling purposes$[kmol/(s\ A)]$. Now,

Table 4.1: constants for model population

Parameter	Value	Unit
N_0	384	-
K_{H2}	8.43e-4	$kmol/(atm\ s)$
$K_{H2}o$	2.81e-4	$kmol/(atm\ s)$
K_{o2}	2.52e-3	$kmol/(atm\ s)$
τ_{H2}	26.1	s
K_{H2}	78.3	s
K_{H2}	2.91	s
r	0.126	ω

$$\frac{d}{dt}\ p_{H2} = \frac{RT}{V_{an}}\ (q_{H2}^{in} - q_{H2}^{out} - 2\ K_r\ I) \tag{4.10}$$

Applying laplace transforms on both sides,we get

$$sp_{H2} - p_{H2}(0) = \frac{RT}{V_{an}} q_{H2}^{in}(s) - q_{H2}^{out}(s) - 2\ K_r\ I \tag{4.11}$$

$$sp_{H2} - p_{H2}(0) = \frac{RT}{V_{an}}(q_{H2}^{in} - 2K_r\ I) - \frac{RT}{V_{an}}(K_{H2}P_{H2}) \tag{4.12}$$

$$(\frac{RT}{V_{an}}K_{H2} + s)P_{H2} = \frac{RT}{V_{an}}(q_{H2}^{in} - 2K_r\ I) \tag{4.13}$$

$$(s + \frac{1}{\tau_{H\,2}})p_{H2} = \frac{1}{\tau_{H2}\ K_{H2}}(q_{H2}^{in} - 2K_r\ I) \tag{4.14}$$

$$\frac{\tau_{H2}s + 1}{\tau_{H2}} p_{H2} = \frac{1}{\tau_{H2}\ K_{H2}}(q_{H2}^{in} - 2K_r\ I) \tag{4.15}$$

$$p_{H2} = \frac{\frac{1}{K_{H2}}}{1 + \tau_{H2}s}(q_{H2}^{in} - 2K_r\ I) \tag{4.16}$$

4.4 Stack Voltage Calculation

For the calculation of stack output voltage we use nernst equation and ohms law. And the expression is as follows,

$$V = N_0(E_0 + \frac{RT}{2F}[ln\frac{p_{H2}\ p_{o2}^{0.5}}{p_{H2}o}]) - r\ I, \tag{4.17}$$

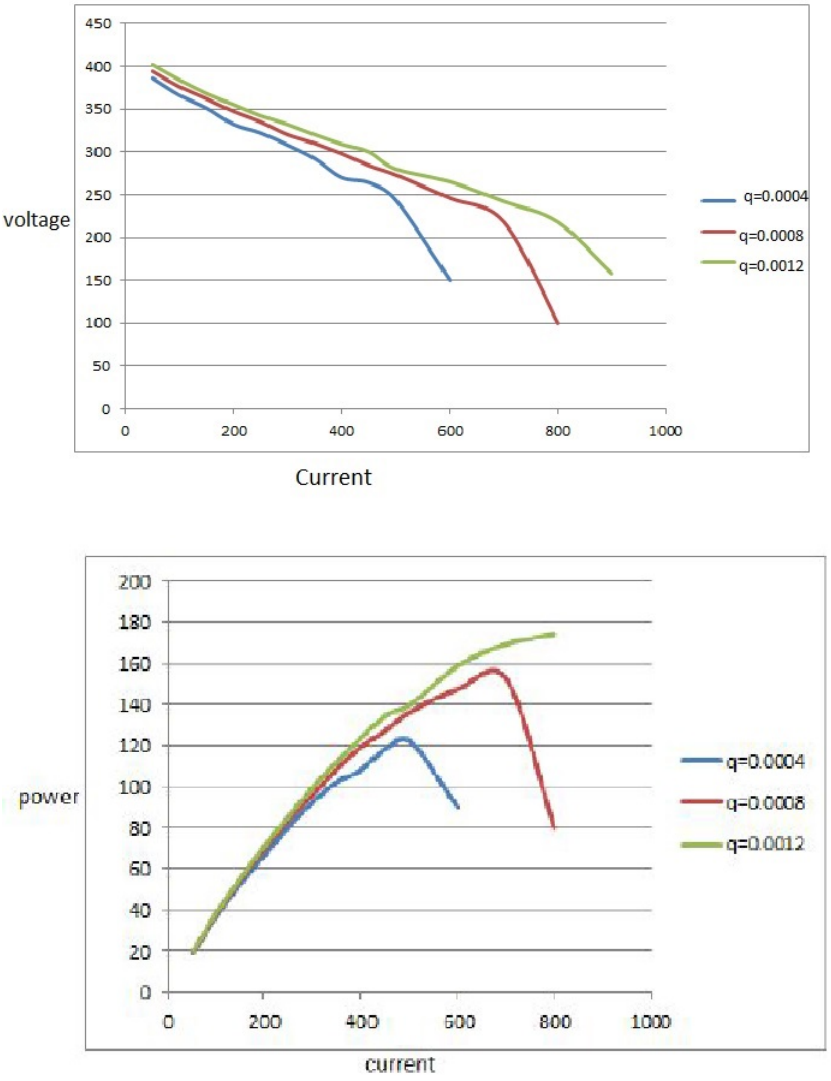

Figure 4.2: Steady state voltage-current and power-current characteristics.

where E_0 is the voltage associated with the free energy[V], R is the universal gas constant $[J/kmol\ K]$, r is the ohmic losses of the stack . The parameters required for the model are listed in table 1. This particular model is used to generate the steady state voltage-current and power-current curves at different flow rates. In this by fixing a current value we run the simulations to get the steady voltage. The same is repeated with different current values to get the v-i plot, are displayed in results.

Chapter 5

Continuous Time Identification From Sampled Data

Most of the dynamic systems are described in the continuous time(differential equations), because the physical laws like conservation equations which explain the system are in the same form.

5.0.1 System Identification Procedure

Consider a linear time- invariant continuous time system with input u and output y can be described by, [12]

$$y(t) = G(p)u(t) + \epsilon(t) \tag{5.1}$$

where G is the transfer function, p is the differential operator for time domain and the term $\epsilon(t)$ represents the disturbances and errors. Here we assume that the input and output are sampled at descrete times $t_1, t_2.....t_N$

Here we have mainly two different kind of models, namely

- Grey-box models : These models are constructed on the basis of physical principles and are generally in continuous time form. Parameters in the model will have a direct physical interpretation. Also known as physically parameterised

models.

- Black-box models : These models can be continuous time or descrete time. Parameters in the model will not have any physical interpretation. These are used to describe the properties of the input output relations of the system.

5.0.2 Least square based state variable filter method

Consider a continuous time model in the form of differential equation

$$\frac{d^n y(t)}{dt^n} + a_1 \frac{d^{n-1} y(t)}{dt^{n-1}} + ... + a_n y(t) = b_0 \frac{d^m y(t)}{dt^m} + b_m u(t) + v(t) \tag{5.2}$$

here $\frac{d^i x(t)}{dt^i}$ represents the i th derivative of the continuous time signal x(t). Now the above equation can be written as

$$y^{(n)}(t) + a_1 y^{n-1}(t) + ... + a_n y(t) = b_0 u^m(t) + ... + b_m u(t) + v(t) \tag{5.3}$$

The equations 2.2 , 2.3 can be written as

$$A(p)y(t) = B(p)u(t) + v(t) \tag{5.4}$$

The above equation can be written for noise free case as

$$A(p)x(t) = B(p)u(t) \tag{5.5}$$

Here x(t) is the noise free output. Now assume that a state variable filter F(p) is applied to both sieds of equation 2.4 , then

$$A(p)F(p)x(t) = B(p)F(p)u(t) \tag{5.6}$$

A minimum order state variable filter F(p) has chosen, will have the form as follows,

$$F(p) = \frac{1}{(p+\lambda)^n} \tag{5.7}$$

where λ is the band width of the filter.

equation 2.6 can be expanded as,

$$(\frac{p^n}{(p+\lambda)^n} + a_1\frac{p^{n-1}}{(p+\lambda)^n} + ... + a_n\frac{1}{(p+\lambda)^n})x(t) = (b_0\frac{p^m}{(p+\lambda)^n} + ... + b_m\frac{1}{(p+\lambda)^n})u(t) \tag{5.8}$$

Let $F_i(p)$ can be defined for a set of filters as,

$$F_i(p) = \frac{p^i}{(p+\lambda)^n} \tag{5.9}$$

Now, using the filter defined in equation 2.7 , equation 2.8 can be written as,

$$(F_n(p) + a_1F_{n-1}(p) + ... + a_nF_0(p))x(t) = (b_0F_m(p) + ... + b_mF_0(p))u(t) \tag{5.10}$$

Now this can be rewritten as,

$$x_f^{(n)}(t) + a_1x_f^{n-1}(t) + ... + a_nx_f^{(0)}(t) = b_0u_f^{(m)}(t) + ... + b_mu_f^{(0)}(t) \tag{5.11}$$

where

$$x_f^{(i)}(t) = f_{(i)}(t) * x(t) \tag{5.12}$$

$$x_f^{(i)}(t) = f_{(i)}(t) * x(t) \tag{5.13}$$

where $f_i(t)$ is the impulse response of the filter and * denotes the convolution operator. Consider a case where additive noise in the output. At a time instant $t = t_k$, substituting $x_f(t)$ for $y_f(t)$, equation 2.11 can be written as in the linear regression form,

$$y_f^{(n)}(t_k) = \varphi_f^T(t_k)\theta + \eta(t_k) \tag{5.14}$$

where ,

$$\varphi_f^T(t_k) = [-y_f^{(n-1)}(t_k)..... - y_f^{(0)}u_f^{(m)}(t_k).....u_f^{(0)}(t_k)] \tag{5.15}$$

$$\theta = [a_1.....a_n b_0....b_m]^T \tag{5.16}$$

Now, the input output signals measured at descrete times $t_1, ..., t_N$ (not necessarily uniformly sampled) from N available samples, The linear least square based state variable filter parameters are given by

$$\theta_{LSSVF} = [\frac{1}{N}\sum_{k=1}^{N}\varphi_f(t_k)\varphi_f^T(t_k)]^{-1}\frac{1}{N}\sum_{k=1}^{N}\varphi_f(t_k)y_f^{(n)}(t_k) \tag{5.17}$$

5.0.3 Refined Instrumental Variable Method

This is an optimal method for the continuous time models and estimation of transfer function models from sampled data. Here dynamic system is modeled in continuous time, while the noise model is estimated as descrete time Auto regressive moving average model. [12]

Problem Formulation

Consider a signle input single output system with input u(t) and noise free output x(t),

$$x^{(n)}(t) + a_1x^{n-1}(t) + ... + a_nx^{(0)}(t) = b_0u^{(m)}(t-\tau) + ... + b_mu^{(t-\tau)}(t) \tag{5.18}$$

where x^i (t) is the ith time derivative of signal x(t) and τ is the time delay.
Now the above equation can be written in transfer function form,

$$x(t) = G_0(p)u(t) = \frac{B_0(p)}{A_0(p)}u(t) \tag{5.19}$$

It is important to consider the errors occured in output measurement. Here the measurement noise is denoted by ξ (t). Now the complete equation can be written as

$$y(t) = G_0(p)u(t) + H_0(p)e_0(t) \tag{5.20}$$

Here our objective is to identify a suitable model stucture and to estimate the parameters which characterize the structure based on the sampling data. $Z^N = u(t_k); y(t_k)$ i=1....N

$$G(p,\rho) = \frac{B(p,\rho)}{A(p,\rho)} = \frac{b_0 p^m + b_1 p^m - 1 + ...b_m}{p^n + a_1 p^{n-1} + ... + a_n} \tag{5.21}$$

And the noise model is as follows,

$$H(q^{-1},\eta) = \frac{C(q^{-1},\eta)}{D(q^{-1},\eta)} = \frac{1 + c_1 q^{-1} + ... + c_q q^{-q}}{1 + d_1 q^{-1} + ... + d_p q^{-p}} \tag{5.22}$$

Here q^{-r} is the backward shift operator. And we need to find out the parameter vector θ for the complete model.

$$\begin{pmatrix} \rho \\ \eta \end{pmatrix}$$

In the simplified refined instrumental variable method, the additive noise is considered to be white. Hence $C(q^{-1},\eta)$ =$D(q^{-1},\eta)$ =1.

Error function is defined according to prediction error minimisation approach, given by

$$\epsilon(t_k) = \frac{D(q^{-1},\eta)}{C(q^{-1},\eta)} y(t_k) - \frac{B(p,\rho)}{A(p,\rho)} u(t_k) \tag{5.23}$$

$$\epsilon(t_k) = \frac{D(q^{-1},\eta)}{C(q^{-1},\eta)} \frac{1}{A(p,\rho)} [A(p,\rho)y(t_k) - \frac{B(p,\rho)}{A(p,\rho)} u(t_k)] \tag{5.24}$$

THe above equation can be written as

$$\epsilon(t_k) = A(p,\rho)y_f(t_k) - B(p,\rho)u_f(t_k) \tag{5.25}$$

Here $y_f(t_k)$, $u_f(t_k)$ are the sampled outputs after continuous time filtering with the filter,

$$f_c(p,\rho) = \frac{1}{A(p,\rho)} \tag{5.26}$$

And the complete model structure can be represented as linear in parameter model,

$$y_f^{(n)}(t_k) = \varphi_f^T(t_k)\theta + \eta(t_k) \tag{5.27}$$

where ,

$$\varphi_f^T(t_k) = [-y_f^{(n-1)}(t_k)..... - y_f^{(0)}u_f^{(m)}(t_k).....u_f^{(0)}(t_k)] \tag{5.28}$$

5.0.4 Estimation Procedure

In this method an iterative algorithm is used, where at each iteration we generate an instumental variable and prefilters. These are updated based on the parameters obtained in the previous iteration.

The instrumental variable is given by

$$\hat{x}(t, \hat{\rho}^{j-1}) = G(p, \hat{\rho}^{j-1})u(t) \tag{5.29}$$

Now, the noise free case of IV vector $\varphi_f^T(t_k)$ is given by

$$\hat{\varphi}_f^T(t_k) = [-\hat{x}_f^{(n-1)}(t_k)..... - \hat{x}_f(t_k)u_f^{(m)}(t_k)]^T \tag{5.30}$$

Now the instrumental variable optimisation problem can be expressed as in the least squares form

$$\hat{\rho}^j(N) = [\sum_{k=1}^{N} \hat{\varphi}_f(t_k)\varphi_f^T(t_k)]^{-1} \sum_{k=1}^{N} \hat{\varphi}_f(t_k)y_f^{(n)}(t_k) \tag{5.31}$$

We have tried these two algorithms, using MATLAB toolbox. Because of the nonlinearities in the system, we were not able to get the exact result.

Chapter 6

Distributed parameter model for SOFC

SOFC is an environmental friendly device to generate electricity with high efficiencies. It has advantages like fuel flexibility, reliability, very low levels of green house gas emissions. Modeling has a huge impact on fuel cell development. Dynamic models are developed inorder to analyze the complicated interactions between the various phenomenon occurring inside the fuel cell. Most of the dynamic models that are available in literature are lumped models. Such that they can only compute average compositions and temperature for a cell or a stack.

Here our objective is to get the dynamic response of the cell to sinusoidal changes in input. In our model the fuel which we use is the product of reformed methane. This model accounts for convective transport in flow channels, porous media diffusion in electrodes, at the interface between electrolyte and electrode and heat transport in flow channels.

6.1 Cell geometry

The model we consider here is the co flow sofc with the cell length of 10cms. The model geometry and assumptions are taken from Zhu [4].

Table 6.1: Cell cimensions

Parameter	Value
air channel	1mm
fuel channel	1mm
anode	500 μ m
cathode	30μ m
electrolyte	20 μ m

6.2 Model assumptions

• The fuel and air which we use are assumed to be ideal because high operating temperature and low pressure is maintained.

• The pressure in the flow channels should be constant.

• The cross section of the fuel cell is very less so that the assumption of plug flow is valid.

• Species transport in the electrode is one dimensional and perpendicular to the channel flow due to the large aspect ratio.

• The temperature variations along the cell thichness van also be neglected due to the large aspect ratios.

6.3 Species transport equation

Here the flow of the gas mixture is assumed to be plug flow. So the species transport equation for the gas mixture in the channel is given by Zhu [4].

$$\frac{\rho\ u\ Y_k}{dx} = \frac{P_e}{A_c} J_k\ M_k \tag{6.1}$$

Where ρ is the density , u is the velocity, Y_k is the mass fraction of the species k, x is the independent coordinate, P_e is the electrochemically active perimeter, A_e is the area of cross section of the flow channel, J_k is the molar flux of the species k, M_k is the molecular weight.

The velocity in the channel calculated from

$$\frac{\rho\ u}{dx} = \frac{P_e}{A_c} J_k\ M_k \tag{6.2}$$

6.4 Energy balance equation

From the energy balance equation the temperature of the gas phace is

$$\rho\ u\ c_p\ \frac{dT}{dx} = \frac{4}{D_h}\ h(T_s - T) \tag{6.3}$$

Where D_h is the hydraulic diameter, h is the heat transfer coefficient, and T_s is the cell temperature. In the same way we can write the transport equations for the gas in electrodes.

6.5 Boundary conditions

The current density i is calculated from modified butler volmer equations for anode and cathode. The Species flux at the interface between electrodes and electrolyte is give by

$J_k = \frac{i}{n_e F}$ n_e is the number of electrons transferred during the reaction, F is the faradays constant.

6.6 Response to sine change in inlet velocity

The step change in the velocity is observed in earlier studies. But here we are interested in sinusoidal change in inlet velocity. Such that the dynamic response in velocity and current is plotted.

In this particular model, after giving the sine change in the inlet velocity, at each time along the length of the cell the velocity is obtained. By collecting all the velocities at the entrance of the cell is plotted against time.

6.7 Wavelet based NARX models for nonlinear system identification

6.7.1 NARX

To describe the relation between input output of a nonlinear system NARX (Nonlinear Autoregressive Moving Avarage model which will have an exogeneous input) method is useful. [13]

Here the current value o the time series is related to the past value of the time series and current, past values of the driving series.

A general NARX model, which is in the form of nonlinear difference equation :

$$y(t) = f(y(t-1), ...y(t-n_y), u(t-1), ..., u(t-n_u)) + e(t) \tag{6.4}$$

where f is an unknown nonlinear mapping and u(t), y(t) are input output samples. e(t) is the noise variable, and n_u , n_y are the maximum input and output lags.

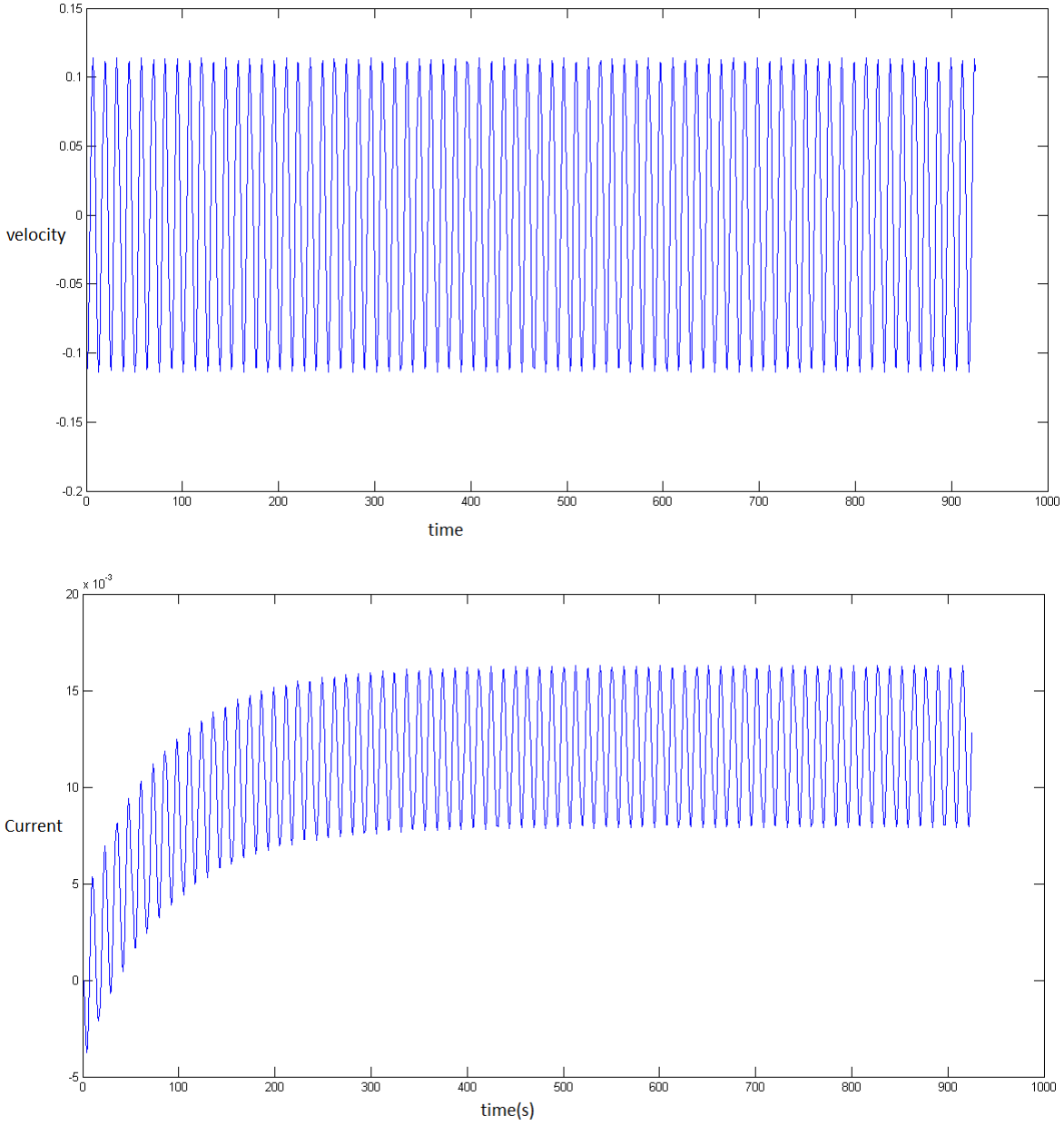

Figure 6.1: Dynamic response of the system with sinusoidal change in inlet velocity.

In NARX model the nonlinear function mapping f is expressed as a finite set of functions which are expanded in terms of lagged input output variables y(t-i), u(t-j). Which is

$$y(t) = f_0 + \sum_{i=1}^{n} f_i(x_i(t)) + \sum_{j=1}^{n} f_{ij}(x_i(t), x_j(t)) + \epsilon(t) \tag{6.5}$$

Expanding functional components of a non parametric NARX model into the wavelet basis. The model becomes linear in parameters and thus can be solved using least square techniques. Here the wavelet analysis adopts a wavelet function called Mother wavelet or simply Wavelets.

where $x_i(t) = y(t-i)$ when i = 1,2,...n_y and $x_i(t) = u(t-i)$ when $i = n_y+1, n_y+2....n$, with $n = n_y + n_u$.

6.7.2 Multiresolution Signal Decomposition

For analyzing the information content of images, multiresolution representation is used as an effective tool. It will provide a complete framework for the Interpretation of the image information at the different resolutions. Bert et al. introduced a pyramidal algorithm for approximating a signal at different resolution. The detais at every resolution 2^j are computed by convolving the original signal with the low pass filter and subsampling the resulting signal. And this operation is repeated over a finite range of resolutions. the details at each resolution are arranged to form a pyramid structure.

Here we talk about an operator which approximates a signal at a resolution 2^j. According to mallat [9] the difference of the information between approximations at different resolutions is extracted by decomposing the signal in a wavelet orthonormal basis. The decomposition is defined as orthogonal multiresolution representation also called as wavelet representation. Where the translations and dilations of a function ψ(x) can be used as expansion of L^2(R) functions. Meyer et al. showed that there

exists a function ψ(x) such that ($\sqrt{2^j}\ \psi(2^j x - k)$) will form an orthonormal basis of L^2(R).

6.7.3 Multiresolution Approximation

An operator A_2^j , approximates a signal at a resolution 2^j . This operator should posses some properties are as follows.

- Consider a function f(x) and $A_2^j f(x)$ is the approximation at a resolution 2^j. Then if we approximate again at same resolution, $A_2^j f(x)$ shold not be changed.
- In all approximated functions at the resolution 2^j, the most similar function to f(x) is $A_2^j f(x)$.
- A signal is approximated at a resolution 2^{j+1} will contain all the information to compute the same signal at a resolution 2^j. A_2^j is a projection operator on V_2^j . $V_2^j \subset V_2^{j+1}$
- The vector spaces of the approximated functions are computed from one another by scaling the approximated function by their resolution value.
- Approximation of a signal at resolution 2^j samples per unit length. If we translate f(x) by a length 2^{-j} , then $A_2^j f(x)$ is also translated by a length proportional to 2^{-j}.

6.7.4 Implementation

The orthogonal projection on V_2^j can be calculated by decomposing the signal f(x) on the orthonormal basis,

$$A_2^j f(x) = 2^{-j} \sum_{n=-\infty}^{+\infty} < f(u), \phi_{2^j}(u - 2^{-j}n) > \phi_2^j(x - 2^{-j}n) \tag{6.6}$$

Let V_2^j is a multiresolution approximation and corresponding scaling function be $\phi(x)$. The functions $(\sqrt{2^{-j-1}}\phi_{2^{j+1}}(x - 2^{-j-1}k\ ))$ form an orthonoraml basis of V_2^{j+1} . Here the function $\phi_{2^j}(u - 2^{-j}n)$ is a memeber of V_2^j also included in V_2^{j+1}. We can expand this in orthonormal basis of V_2^{j+1}

$$\phi_{2^j}(u - 2^{-j}n) = 2^{-j-1} \sum_{k=-\infty}^{+\infty} < \phi_{2^j}(u - 2^{-j}n), \phi_2^{j+1}(u - 2^{-j-1}k) > .\phi_2^{j+1}(x - 2^{-j-1}k) \tag{6.7}$$

After changing the variables in the inner product integral, it can be written as,

$$2^{-j-1} < \phi_{2^j}(u - 2^{-j}n), \phi_2^{j+1}(u - 2^{-j-1}k) >=< \phi_2^{-1}, \phi(u - (k - 2n)) > \tag{6.8}$$

Now, computing the inner products of f(x) with both sides of

$$< f(u), \phi_{2^j}(u - 2^{-j}n) >= \sum_{k=-\infty}^{+\infty} < \phi_{2^{-1}}(u - (k - 2n)) > . < f(u), \phi_2^{j+1}(u - 2^{-j-1}k) > \tag{6.9}$$

Introducing a mirror filter (H), with impulse response $\tilde{h}$(n)=h(-n).

$$h(n) =< \phi_{2^{-1}}(u - n) > \tag{6.10}$$

Now, by inserting this in previuos equation, we get

$$< f(u), \phi_{2^j}(u - 2^{-j}n) >= \sum_{k=-\infty}^{+\infty} h(k - 2n). < f(u), \phi_2^{j+1}(u - 2^{-j-1}k) > \tag{6.11}$$

Approximation of a function at a resolution 2^j can be computed by convolution of approximation at resolution 2^{j+1} with filter H and downsampling the output. All the discrete approximations at resolutions lessthan j are computed by repeating the process. This procedure is called pyramid transform.

6.7.5 Detail Signal

In this section extraction of the information between two approximation at resolutions 2^{j+1} and 2^j. Here the difference is called detail signal. Now the detail signal at a resolution 2^j is the orthogonal projection of original signal on the orthogoanl complement of V_2^j in V_2^{j+1}. Here O_2^j is the orthogonal complement. Now let V_2^j is a multiresolution approximation vector space. ϕ(x) is the scaling function and ψ(x) be the corresponding wavelet. Translations and dilations of this function ψ(x) will form orthonormal basis of O_2^j.

Let the orthogonal projection on vector space O_2^j is $P_{O_{2^j}}$, can be written as

$$P_{O_{2^j}} f(x) = 2^{-j} \sum_{n=-\infty}^{+\infty} < f(u), \psi_{2^j}(u - 2^{-j}n) > \psi_2^j(x - 2^{-j}n) \tag{6.12}$$

Here the function $\psi_{2^j}(x - 2^{-j}n)$ is a memeber of O_2^j also included in $V_2^j + 1$. We can expand this in orthonormal basis of V_2^{j+1}

$$\psi_{2^j}(x - 2^{-j}n) = 2^{-j-1} \sum_{k=-\infty}^{+\infty} < \psi_{2^j}(u - 2^{-j}n), \phi_2^{j+1}(u - 2^{-j-1}k) > .\phi_2^{j+1}(x - 2^{-j-1}k) \tag{6.13}$$

And the detail signal D_{2^j} f can be computed with convolution of $A_{2^{j+1}}$ with a filter G and downsampling the output. Decomposition of a discrete approximation $A_{2^{j+1}}$f into the approximations at lower resolutions and detail signals D_{2^j} f can be shown in following figure.

6.7.6 Multiresolution approximation for two variable case

Let V_{2^j} is a multiresolution approximation of $L^2(R^2)$ and the associated scaling function $\phi(x, y)$ can be $\phi(x, y) = \phi(x)\phi(y)$. The orthonormal basis of V_{2^j} will be formed by family of functions $(2^{-j}\phi_{2^j}(x - 2^{-j}n, (y - 2^{-j}m))$. And ψ(x) be the wavelet associated with the scaling function ϕ(x). Orthonormal basis of O_2^j formed by three

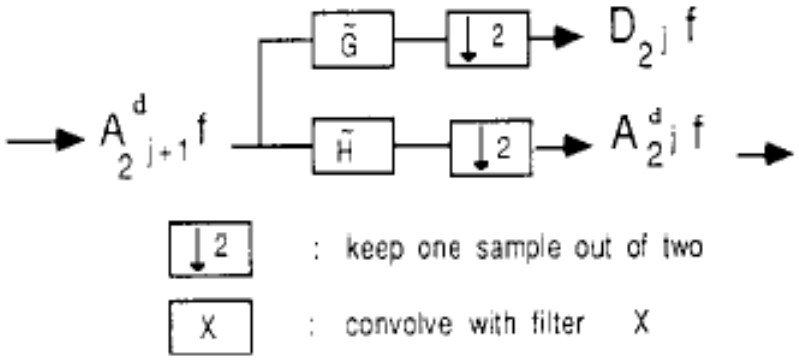

Figure 6.2: Signal decompostion

wavelets, they are

$$\psi^1(x,y) = \phi(x)\ \psi(y) \tag{6.14}$$

$$\psi^2(x,y) = \psi(x)\ \phi(y) \tag{6.15}$$

$$\psi^3(x,y) = \psi(x)\ \psi(y) \tag{6.16}$$

And the difference of the information between approximations at 2^{j+1} and 2^j are given by

$$D^1_{2^j} f = (< f(x,y), \psi^1_{2^j}(x - 2^{-j}n, (y - 2^{-j}m) \tag{6.17}$$

$$D^2_{2^j} f = (< f(x,y), \psi^2_{2^j}(x - 2^{-j}n, (y - 2^{-j}m) \tag{6.18}$$

$$D^3_{2^j} f = (< f(x,y), \psi^3_{2^j}(x - 2^{-j}n, (y - 2^{-j}m) \tag{6.19}$$

The two dimensional signal decompostion can be shown in figure.

6.8 Conclusions

In this work, we have studied the system identification techniques. First, we got the data from a detailed distributed parameter model, where a sinusoidal change in inlet velocity was given as input and the corresponding output response is teken

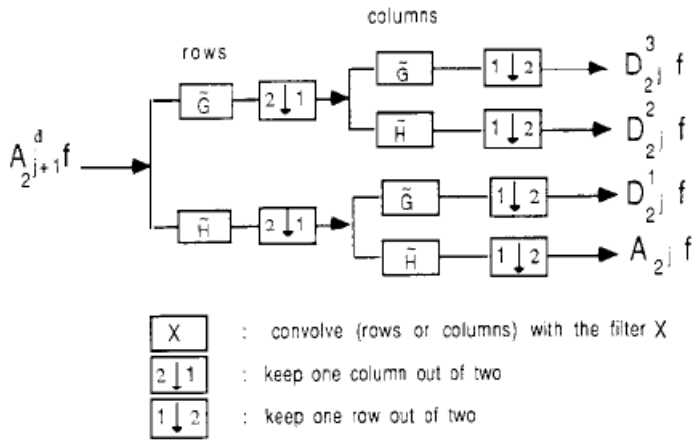

Figure 6.3: Two dimensional Signal decompostion

as output. We have tried the continuous time identification techniques like Linear least square state variable filter method and Simplified refined instrumental variable method because the input output data that we chose is nonuniformly sampled. But these algorithms did not give us good results. Then we tried Nonlinear system identification techniques like NARX. Where first we implemented using mexican hat wavelets, later on we extended this to multiresolution alalysis.

References

[1] S. Kakac, A. Pramuanjaroenkij, and X. Y. Zhou. A review of numerical modeling of solid oxide fuel cells. *International journal of hydrogen energy* 32, (2007) 761–786.

[2] V. M. Janardhanan and O. Deutschmann. Modeling of solid-oxide fuel cells. *Zeitschrift für Physikalische Chemie* 221, (2007) 443–478.

[3] E. Achenbach. Three-dimensional and time-dependent simulation of a planar solid oxide fuel cell stack. *Journal of power sources* 49, (1994) 333–348.

[4] H. Zhu, R. J. Kee, V. M. Janardhanan, O. Deutschmann, and D. G. Goodwin. Modeling elementary heterogeneous chemistry and electrochemistry in solid-oxide fuel cells. *Journal of the electrochemical society* 152, (2005) A2427–A2440.

[5] A. M. Colclasure, B. M. Sanandaji, T. L. Vincent, and R. J. Kee. Modeling and control of tubular solid-oxide fuel cell systems. I: Physical models and linear model reduction. *Journal of Power Sources* 196, (2011) 196–207.

[6] B. M. Sanandaji, T. L. Vincent, A. M. Colclasure, and R. J. Kee. Modeling and control of tubular solid-oxide fuel cell systems: II. Nonlinear model reduction and model predictive control. *Journal of Power Sources* 196, (2011) 208–217.

[7] J. Arriagada, P. Olausson, and A. Selimovic. Artificial neural network simulator for SOFC performance prediction. *Journal of Power Sources* 112, (2002) 54–60.

[8] F. Jurado. A method for the identification of solid oxide fuel cells using a Hammerstein model. *Journal of Power Sources* 154, (2006) 145–152.

[9] S. G. Mallat. A theory for multiresolution signal decomposition: the wavelet representation. *Pattern Analysis and Machine Intelligence, IEEE Transactions on* 11, (1989) 674–693.

[10] P. Van Overschee and B. De Moor. Subspace identification for linear systems: TheoryImplementationApplications. Springer Science & Business Media, 2012.

[11] J. Padulles, G. Ault, and J. McDonald. An integrated SOFC plant dynamic model for power systems simulation. *Journal of Power sources* 86, (2000) 495–500.

[12] H. Garnier, M. Mensler, and A. Richard. Continuous-time model identification from sampled data: implementation issues and performance evaluation. *International Journal of Control* 76, (2003) 1337–1357.

[13] H.-L. Wei, S. A. Billings, and M. A. Balikhin. Wavelet based non-parametric NARX models for nonlinear input–output system identification. *International journal of systems science* 37, (2006) 1089–1096.